Autophagy Induced by Calcium Phosphate Precipitates Targets Damaged Endosomes*

Xi Chen[‡§], Bilon Khambu[§], Hao Zhang[§], Wentao Gao[¶], Min Li[§‖], Xiaoyun Chen[§], Tamotsu Yoshimori[**], and Xiao-Ming Yin[§1]

From the ‡Children's Hospital, Zhejiang University School of Medicine, Hangzhou, Zhejiang 310000, China, the §Department of Pathology and Laboratory Medicine, Indiana University School of Medicine, Indianapolis, Indiana 46202, the ¶Department of Surgery, University of Pittsburgh School of Medicine, Pittsburgh, Pennsylvania 15261, the ‖Department of Pharmacology and Toxicology, School of Pharmaceutical Sciences, Sun Yat-sen University, Guangzhou 510006, China, and the **Department of Genetics, Osaka University, Suita, Osaka 565-0871, Japan

Background: Relationship of autophagosomes with endosomal vesicles varies in different conditions.
Results: Calcium phosphate precipitates required endocytosis to induce autophagy, caused endosome damage, and recruited autophagosomes to the damaged vesicles.
Conclusion: Damaged endosomes can be targeted by autophagosomes.
Significance: Autophagy may play a role in endosomal homeostasis.

Calcium phosphate precipitates (CPPs) form complexes with DNA, which enter cells via endocytosis. Under this condition CPPs induce autophagy via the canonic autophagy machinery. Here we showed that CPP-induced autophagy was also dependent on endocytosis as the process was significantly inhibited by methyl-β-cyclodextrin and dynasore, which suppress clathrin-dependent endocytosis. Consistently, CPP treatment triggered the formation of filipin-positive intracellular vesicles whose membranes are rich in cholesterol. Unexpectedly, these vesicles were also positive for galectin 3, suggesting that they were damaged and the membrane glycans became accessible to galectins to bind. Endosome damage was caused by endocytosis of CPPs and was reversed by calcium chelators or by endocytosis inhibitors. Notably, CPP-induced LC3-positive autophagosomes were colocalized with galectin 3, ubiquitin, and p62/SQSTM1. Inhibition of galectin 3 reduced p62 puncta and autophagosome formation. Knockdown of p62 additionally inhibited the colocalization of autophagosomes with galectins. Furthermore, most of the galectin 3-positive vesicles were colocalized with Rab7 or LAMP1. Agents that affect endosome/lysosome maturation and function, such as bafilomycin A_1, also significantly affected CPP-induced tubulovesicular autophagosome formation. These findings thus indicate that endocytosed CPPs caused endosome damage and recruitment of galectins, particularly at the later endosome stage, which led to the interaction of the autophagosomal membranes with the damaged endosome in the presence of p62.

As an evolutionarily conserved cellular degradation mechanism, macroautophagy, hereafter referred to as autophagy, can be induced by various physiological and pathological stimuli (1). A cascade of autophagy-related (Atg)[2] proteins is engaged for the formation of double-membraned autophagosomes, which eventually fuse with lysosomes for degradation of the contents (2).

Calcium-mediated DNA transfection is the first method developed to introduce DNA into mammalian cells (3). Under the proper condition, calcium phosphate forms precipitates, which bind to DNA molecules. We and others have found that the transfection process induced a transient activation of autophagy, which depends on calcium phosphate precipitates (CPPs) but not DNA (4, 5). CPPs induce autophagy via the canonical autophagy machinery without affecting mTORC1 activity (4, 6, 7). In addition, the biogenesis of CPP-induced autophagosome is related to endoplasmic reticulum, but not to the Golgi complex or the mitochondria (7).

Matured autophagosomes can be identified by the presence of Atg8 in yeast cells, or one of the homologues in mammalian cells, such as microtubule-associated protein 1 light chain 3 (LC3). These molecules are conjugated to phosphatidylethanolamine in autophagosomal membranes and are crucial to the expansion and completion of the autophagosomal vesicles that enwrap subcellular materials for degradation (8). LC3-labeled autophagosomal structure can be measured for determining the level of autophagy activity and for identifying subcellular structures interacting with the autophagosomes based on colocalization (9).

CPP-induced autophagy is characterized by elaborately developed LC3-positive puncta that can manifest both tubular and vesicular morphology, known as LC3-positive tubulovesicular structures (LC3-TVS) (6). These structures are reminiscent of the endosomal network, raising the possibility that CPP-induced autophagosomes may have significant interactions

---

[2] The abbreviations used are: Atg, autophagy-related; BafA$_1$, bafilomycin A$_1$; ConA, concanamycin A; CPP, calcium phosphate precipitate; Gal3, galectin 3; LC3, light chain 3; LC3-TVS, LC3-positive tubulovesicular structures; MβCD, methyl-β-cyclodextrin; v-ATPase, vacuolar H$^+$-ATPase.
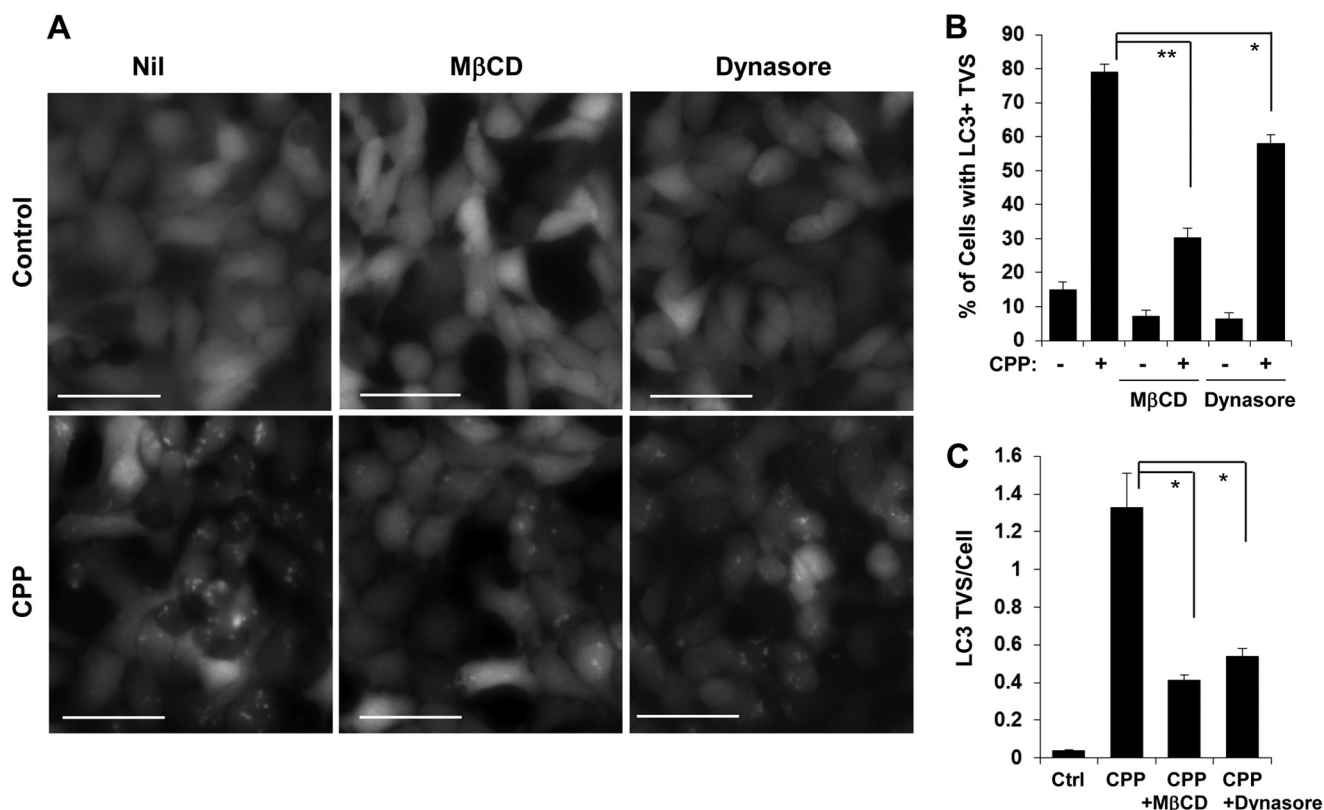
FIGURE 1. **CPP-induced autophagy requires clathrin-dependent endocytosis.** HEK293 cells expressing GFP-LC3 were cultured with MβCD (10 mM) or dynasore (50 μM) for 30 min before CPPs were added for another 4 h. GFP-LC3-TVS were imaged (*A*) and quantified (*B* and *C*). *Scale bars*, 50 μm. *Error bars*, S.E.

with endosomal vesicles. To explore this hypothesis we examined in this study the importance of endocytosis to CPP-induced autophagy, the impact of CPPs on the integrity of the endosomal vesicles, the relationship of the CPP-induced autophagosomes with endosomes, and the effect of the endosome/lysosome function on the formation of CPP-induced autophagosome.

EXPERIMENTAL PROCEDURES

Antibodies—The following antibodies were used: anti-p62/SQSTM1 (Santa Cruz Biotechnology, sc-28359), anti-ubiquitin (Santa Cruz Biotechnology, sc-8017), anti-galectin 3 (Covance, MMS-5004), anti-LAMP1 and anti-LAMP2 (Developmental Studies Hybridoma Bank, Iowa City, IA). Secondary antibodies were conjugated to Cy3 (Jackson ImmunoResearch, West Grove, PA) or Alexa Fluor 488 (Invitrogen).

Cell Culture, Plasmids, and Transfection—HEK293 (ATCC, CRL-1573) were cultured in DMEM supplemented with 10% fetal bovine serum, at 37 °C with 5% CO$_2$. CPPs were prepared by mixing equal volumes of CaCl$_2$ (256 mM) and buffer A (50 mM HEPES, 3 mM Na$_2$HPO$_4$, pH 7.05,) as described previously (4) and were administrated dropwise to cells at 20% (v/v) for 4 h unless otherwise indicated. To visualize transfected DNA in cells, plasmid DNA (pDsRed, 25–50 μg), SYBR Green, or propidium iodide (1 μg/ml final concentration) was admixed with CaCl$_2$ solution (256 mM) before adding to buffer A as described previously (10). The CPP-DNA complex was then introduced to cells as in the case of CPPs alone. DNA was visualized by

fluorescence microscopy. BAPTA-AM (10 μM), methyl-β-cyclodextrin (MβCD; 2.5–10 mM), or dynasore (50 μM) was added 30 min before, and DQ Red BSA (1 μg/ml, Invitrogen) was added 2 h before CPP treatment and was continuously present through the treatment. Bafilomycin A$_1$ (BafA$_1$; 100 nM), concanamycin A (ConA; 200 μM), chloroquine (50 μM), or NH$_4$Cl (2.5 mM) was added concomitantly with CPPs and remained in the culture through the treatment.

Turbofect (Fermentas, Pittsburgh, PA) was used for transfection of mCherry-galectin 3 (11) and GFP-Rab7 (6), as described previously. A pool of siRNA for galectin 3 (Santa Cruz, sc-155994) or p62/SQSTM1 (Santa Cruz, sc-29679) was transfected (100 pmol/well of a 24-well plate) into HEK293 cells constitutively expressing GFP-LC3 using Lipofectamine RNAiMAX (Invitrogen). A negative siRNA (Invitrogen 1007792) was used as a control. Forty-eight hours after transfection cells were treated with CPPs and analyzed.

Immunofluorescence Staining and Fluorescence Microscopy—Cells were cultured on glass slides, fixed with 4% paraformaldehyde, permeabilized with 0.2% Triton X-100, and blocked with 2% BSA before incubation with the indicated antibodies. Cells were costained with Hoechst 33342 for the nucleus. Alternatively, fixed cells were incubated with filipin (0.1 mg/ml; Cayman Chemicals, Ann Arbor, MI) without permeabilization for 4 h. Fluorescence microscopy was carried out with a Nikon Eclipse TE200 microscope with the NIS-Elements software. Confocal microscopy was carried out with PerkinElmer Life
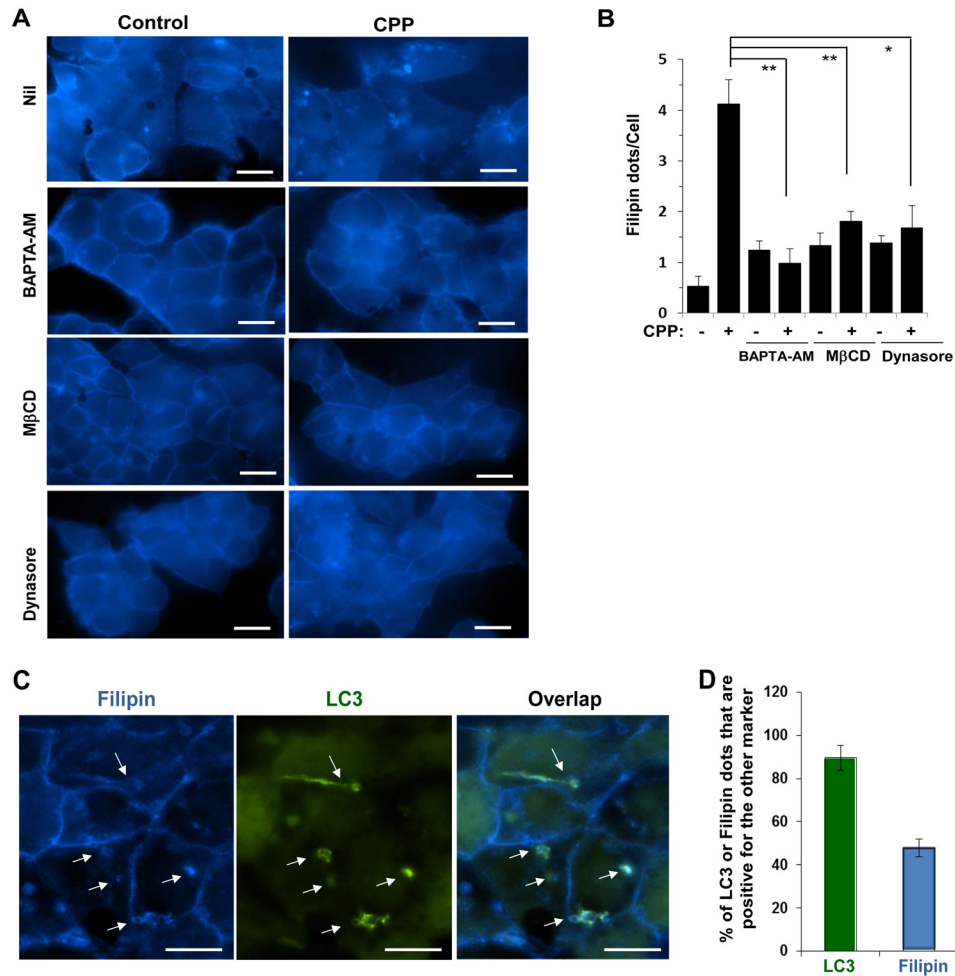
FIGURE 2. **CPPs induce filipin-positive puncta in an endocytosis-dependent manner.** *A* and *B*, HEK293 cells were cultured with BAPTA-AM (10 μM), MβCD (2.5 mM), or dynasore (50 μM) for 30 min followed by CPP treatment for 4 h. Cells were then fixed and stained with filipin. Images were taken immediately (*A*), and filipin-positive puncta per cell were quantified (*B*). *C* and *D*, HEK293 cells expressing GFP-LC3 were treated with CPPs for 4 h, fixed, stained with filipin, and imaged. *Arrows* indicate puncta with both GFP-LC3 and filipin signals (*C*). The percentages of LC3- or filipin-positive puncta that were also positive for the other marker were determined (*D*). **, $p < 0.01$; *, $p < 0.05$. *Scale bars*, 10 μm. *Error bars*, S.E.

Sciences R2-E2 equipped with Andor iQ software for colocalization studies. Images were processed with NIS-Elements or ImageJ software.

Statistical Analysis—For quantification of vesicular structures, at least three optical fields with >50 cells/experimental condition from three or more experiments were analyzed. Data shown are mean ± S.E. and were evaluated by *t* test or one-way analysis of variance using Excel or SigmaStat 3.5. $p < 0.05$ was considered significant.

RESULTS

CPP-induced Autophagy Depends on Clathrin-mediated Endocytosis—The CPP-DNA complex enters cells via endocytosis (12, 13). To determine whether CPP-induced autophagy was affected by endocytosis we cotreated cells with CPPs and chemicals that affect endocytosis. By depleting cholesterol from the plasma membrane, MβCD strongly inhibits clathrin-dependent endocytosis because cholesterol-enriched lipid domains are necessary for the invagination of clathrin-coated pits (14, 15). Dynasore is a potent inhibitor of dynamin, which is essential for clathrin-dependent coated vesicle formation during endocytosis (16, 17). We found that CPP-induced LC3-TVS were significantly inhibited by MβCD and by dynasore (Fig. 1, *A–C*). Thus, CPP-induced autophagy required clathrin-dependent endocytosis.

Staining cells with filipin, a dye specific for cholesterol (18), allowed us to detect intracellular filipin-positive dots in CPP-treated cells (Fig. 2, *A* and *B*), which were suppressed by MβCD or dynasore, suggesting that these dots represented endocytosed vesicles. Interestingly, these filipin-positive puncta could be also suppressed by BAPTA-AM, a cell-permeable calcium chelator. We had shown previously that BAPTA-AM was able to inhibit CPP-induced LC3-TVS (4, 7). Thus the present finding suggested that BAPTA-AM might suppress autophagy at an early stage by inhibiting CPPs to enter cells via endocytosis. It may suppress any subsequent steps requiring calcium as well.

The importance of endocytosis to CPP-triggered autophagy was further confirmed by the observation that the LC3 signal was often colocalized with the filipin signal (Fig. 2, *C* and *D*). Nearly 90% of LC3-TVS were positive for filipin staining, although only 48% of filipin signal was overlapped with that of LC3, implying that filipin-positive vesicles could interact with LC3-positive autophagosomes.
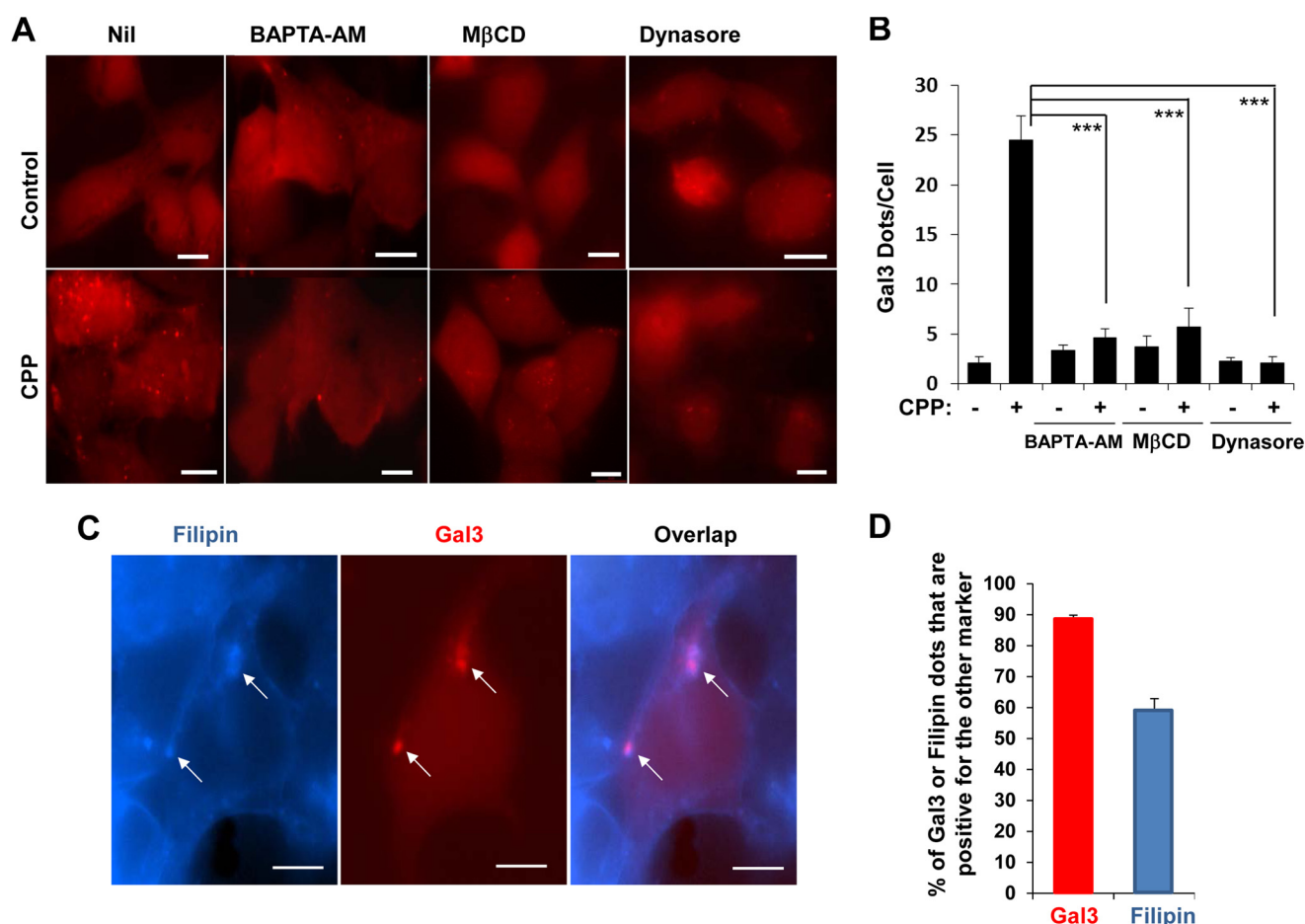
FIGURE 3. **CPP-induced endosome damage is dependent on calcium and endocytosis.** *A* and *B*, HEK293 cells expressing mCherry-Gal3 were cultured with BAPTA-AM (10 μM), MβCD (10 mM), or dynasore (50 μM) for 30 min followed by CPP treatment for 4 h. mCherry-Gal3-positive puncta were imaged (*A*) and quantified (*B*). *C* and *D*, alternatively, CPP-treated cells were fixed and stained with filipin followed by imaging. *Arrows* indicate puncta with both mCherry-Gal3 and filipin signals (*C*). The percentages of Gal3- or filipin-positive dots that were also positive for the other marker were determined (*D*). ***, $p < 0.001$. *Scale bars*, 10 μm. *Error bars*, S.E.

CPP-induced Endosome Damage Correlates with the Interaction with the LC3-positive Autophagosomes—Endocytosis can be linked to autophagy activation. The best examples are known in the cellular defense against certain intracellular bacteria (19). Phagocytosed bacteria trigger an autophagy process, which results in the formation of a LC3-positive autophagosome-like structure that surrounds the bacteria-containing vesicles (20, 21). This structure is responsible for the effective clearance of the phagocytosed bacteria through lysosome-mediated degradation. Notably, endosomal vesicles containing phagocytosed bacteria exposed glycans because of vesicle lysis (22, 23). Glycans are normally present only on cell surface and in the lumens of endocytic compartments (24), and would not be accessible to the cytosolic galectins. Glycans on damaged endomembranes become accessible to and bound by the cytosolic galectins, including galectin 3, 8, or 9 (22, 23). This galectin-glycan interaction seems to be critical for the anti-bacteria autophagy (23).

Sterile damage to endosomes by osmotic shock (23) and to lysosomes by certain lysosomotropic agents (11) can also trigger galectin recruitment to the damaged vesicles, followed by autophagic engulfment. To determine whether CPPs could cause sterile damage to vesicles of the endosomal system, thus

leading to interaction with the autophagosome, we examined whether CPP treatment could result in galectin recruitment to the vesicle. Using mCherry-galectin 3 (Gal3) as the probe, we found that CPP treatment induced Gal3-positive puncta, which were dependent on calcium and clathrin-dependent endocytosis (Fig. 3, *A* and *B*). Thus, the intracellular calcium chelator, BAPTA-AM, and endocytosis inhibitors, MβCD and dynasore, inhibited Gal3 puncta formation. In addition, most of the Gal3-positive vesicles were overlapped with the filipin signal, whereas approximately 60% of filipin-positive vesicles were positive for Gal3 (Fig. 3, *C* and *D*). These results suggested that CPPs caused damages to the endosomal membranes and exposure of glycans, which subsequently became recognized by galectins.

To determine whether transfected DNA could be found in the damaged vesicles, we labeled a DNA construct with DNA-binding fluorescent dye and transfected it into cells via CPPs. The labeled DNA was found inside cells and could be colocalized with Gal3 puncta (Fig. 4*A*), suggesting that DNA resided in the endocytic vesicles that exposed glycans. Notably, DNA could also be found in colocalization with LC3-TVS (Fig. 4*B*), suggesting that the endocytosed DNA were engulfed by autophagosomes. Supporting the latter possibility, Gal3 signals
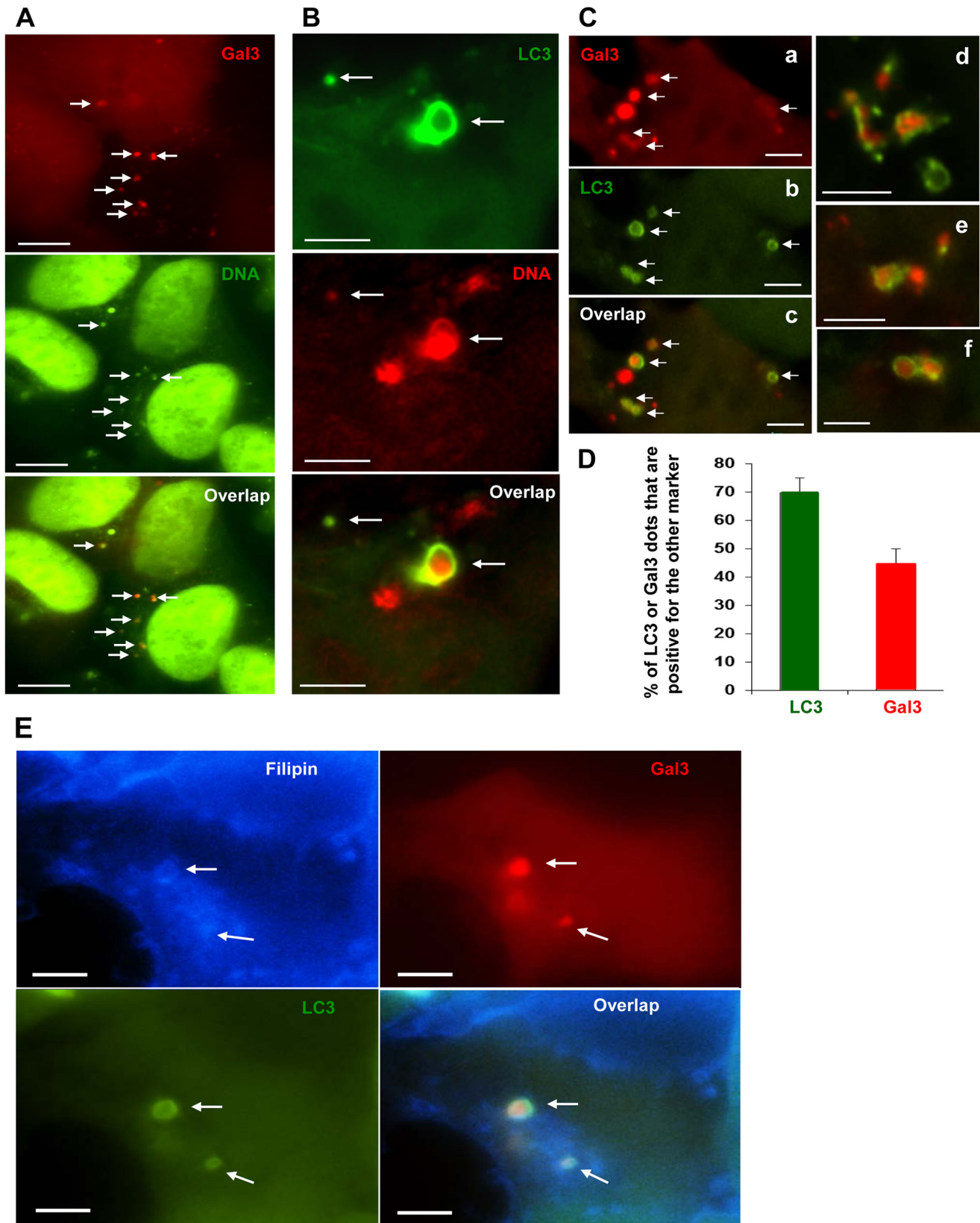
FIGURE 4. **Transfected DNA is colocalized with damaged endosomes and autophagosomes.** *A*, HEK293 cells expressing mCherry-Gal3 were transfected with SYBR-Green-labeled DNA mediated by CPPs. *Arrows* indicate overlapped signals of CPP-induced Gal3 puncta and transfected DNA. *B*, HEK293 cells expressing GFP-LC3 were transfected with propidium iodide-labeled DNA mediated by CPPs. *Arrows* indicate overlapped signals of CPP-induced LC3-TVS and transfected DNA. *C* and *D*, HEK293 cells expressing both GFP-LC3 and mCherry-Gal3 were treated with CPPs for 4 h. Images were then taken (*C*), and the percentages of LC3- or Gal3-positive dots that were also positive for the other marker were calculated (*D*). *E*, cells were fixed and stained by filipin and imaged. Puncta positive for all three markers are indicated by *arrows*, which show vesicles with overlapped signals. *Scale bars*, 10 μm (*A*) and 5 μm (*B, C,* and *E*). *Error bars*, S.E.
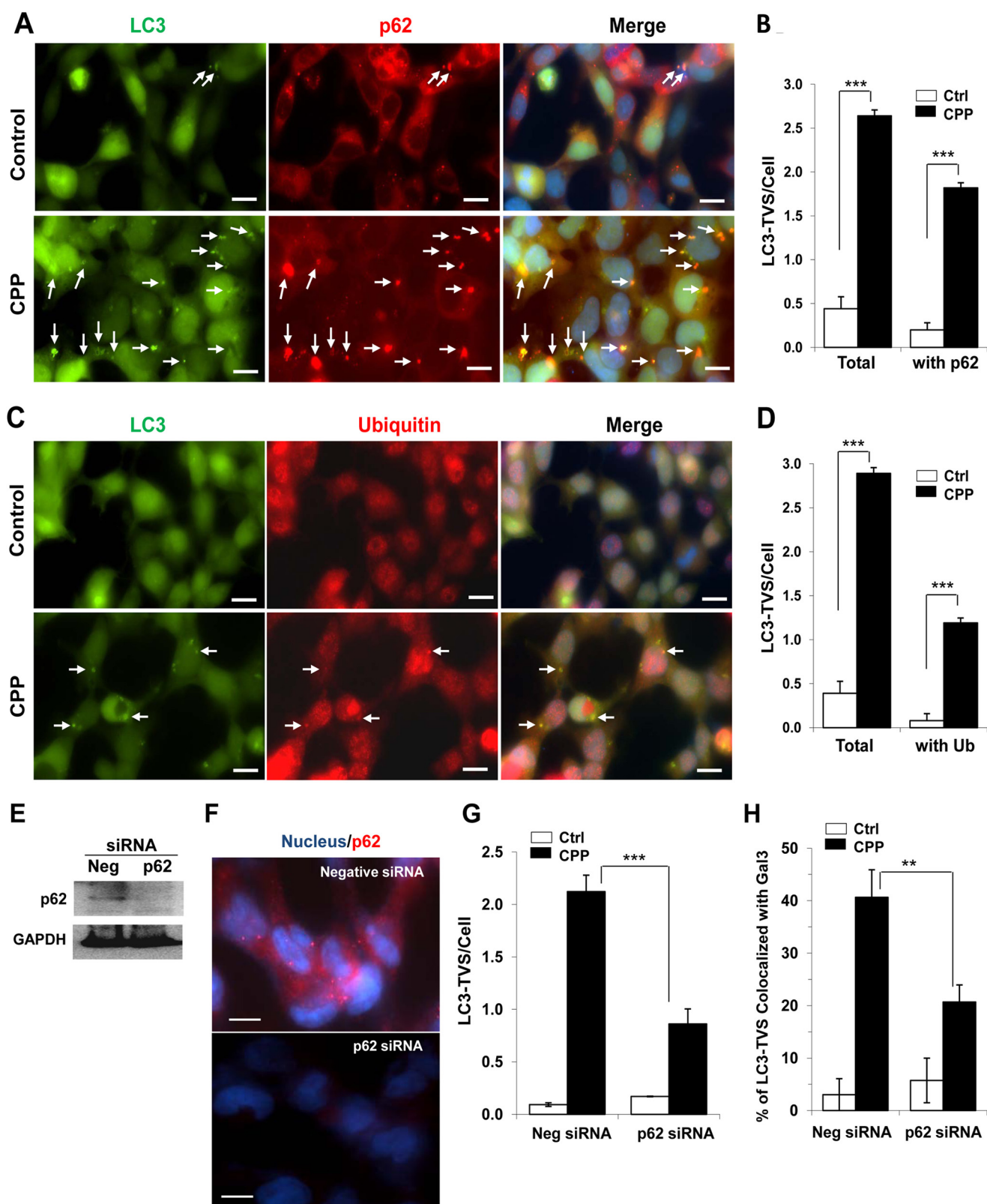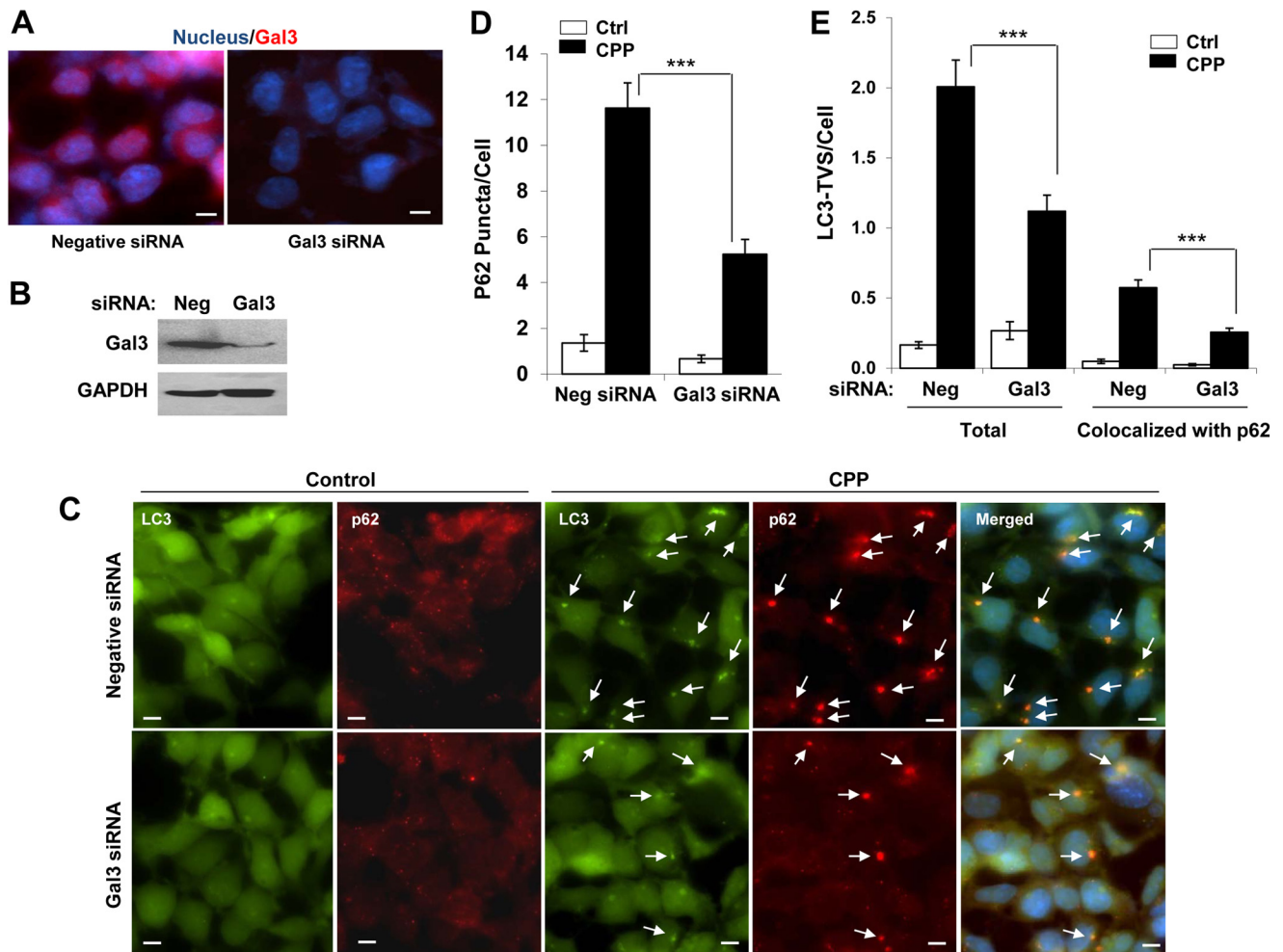
FIGURE 5. **Inhibition of p62 affects the formation of LC3-TVS and the colocalization with Gal3.** *A–D*, GFP-LC3-expressing HEK293 cells were treated with or without CPPs for 4 h, fixed, and stained with anti-p62 (*A* and *B*) or ubiquitin (*C* and *D*) and counterstained with Hoechst 33342 for the nucleus. Images were taken (*A* and *C*), and the total number of LC3-TVS/cell and those that were colocalized with p62 (*B*) or ubiquitin (*D*) were quantified. *Arrows* indicate overlapped signals of LC3 and p62. *E* and *F*, HEK293 cells were transfected with negative or p62-specific siRNA for 48 h. Cells were harvested for Western blot analysis of p62 protein level (*E*). Alternatively, cells were fixed and immunostained for p62 and counterstained with Hoechst 33342 for the nucleus (*F*). *G* and *H*, HEK293 cells expressing GFP-LC3 were transfected with siRNA as above and then treated with or without CPPs for 4 h, followed by fixation and staining with anti-Gal3. The number of LC3-TVS (*G*) and the percentage of LC3-TVS that were colocalized with Gal3 (*H*) were quantified. *Scale bars*, 10 μm. ***, $p < 0.001$; **, $p < 0.01$. *Error bars*, S.E.

FIGURE 6. Inhibition of Gal3 affects the formation of p62 puncta and LC3-TVS. *A* and *B*, GFP-LC3-expressing HEK293 cells were transfected with negative or Gal3-specific siRNA for 48 h. Cells were fixed and immunostained for Gal3 and counterstained with Hoechst 33342 for the nucleus (*A*). Alternatively, cells were harvested for Western blot analysis of Gal3 protein level (*B*). *C–E*, 48 h after transfection with negative or Gal3-specific siRNA, GFP-LC3-expressing HEK293 cells were treated with or without CPPs for 4 h, followed by fixation, staining with anti-p62, and counterstaining with Hoechst 33342 (*C*). The number of p62 puncta (*D*) and LC3-TVS (total and those colocalized with p62) (*E*) were quantified. *Arrows* indicate overlapped signals of LC3 and p62. *Scale bars*, 10 μm. ***, $p < 0.01$. *Error bars*, S.E.

were found to be colocalized with LC3 signals (Fig. 4, *C* and *D*). In cells expressing GFP-LC3 and mCherry-Gal3, we found that as many as 70% of LC3-TVS were positive for Gal3 whereas 45% of Gal3-positive vesicles were positive for LC3. This suggested that a majority of LC3-positive autophagosomes interacted with Gal3-positive damaged endosomal vesicles although not all of the latter were engaged in this interaction at a given time point. In addition, LC3/Gal3 double positive vesicles were frequently positive for filipin (Fig. 4*E*), suggesting that the processes represented by the three markers were closely linked. It is likely that the CPP entrance caused damages to the endosomal vesicles, which led to the recruitment of galectins and interaction of the autophagosomal compartment.

P62 and Gal3 Affect LC3-positive Autophagosome Formation— Selective autophagy has developed multiple modes for autophagosomes to recognize specific targets. Ubiquitination of the targets followed by the recruitment of p62 provides one of the mechanisms to recruit autophagosomal components (25). Indeed, we found that a large percentage of CPP-induced LC3-TVS were colocalized with p62 and ubiquitin (Fig. 5, *A–D*). To

investigate further the possible role of p62 in recruiting LC3-TVS, we knocked down p62 (Fig. 5, *E* and *F*) and found that CPP-induced formation of LC3-TVS was significantly reduced (Fig. 5*G*). In addition, inhibition of p62 also significantly reduced the colocalization of Gal3 and LC3 (Fig. 5*H*), suggesting the role of p62 in recruiting LC3 to Gal3-positive endosomes.

The data supported a model in which Gal3 on the damaged endosomes might be instrumental in recruiting p62 and then LC3 to form autophagosomes. We therefore inhibited the expression of Gal3 using specific siRNA (Fig. 6, *A* and *B*). We found that knockdown of Gal3 indeed resulted in a reduction of p62 puncta (Fig. 6*C*), the total number of LC3-TVS, and the number of LC3-TVS that was colocalized with p62 (Fig. 6*D*), supporting the proposed model.

*Damaged Endosomal Membranes That Interact with Autophagosomes Represent Mainly Later Endosomes and/or Lysosomes—*Endocytosed vesicles would mature along the general endosome pathway. To determine whether the stage of maturation affected Gal3 recruitment we examined common endo-
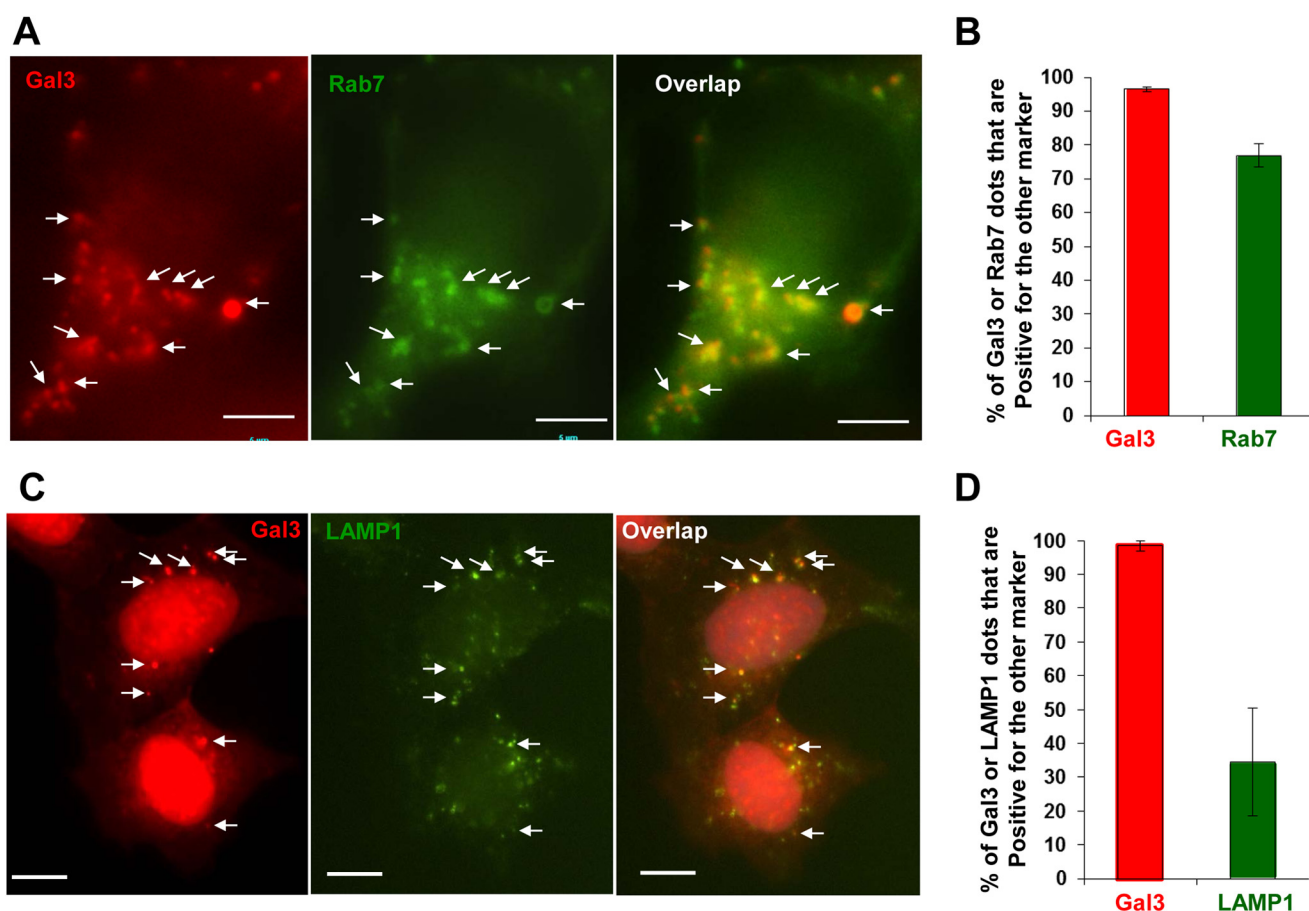
FIGURE 7. **Gal3 signals are colocalized with Rab7 and LAMP1.** *A* and *B*, HEK293 cells expressing mCherry-Gal3 and GFP-Rab7 were treated with CPPs for 4 h. Images were taken (*A*). The percentages of Gal3- or Rab7-positive dots that were also positive for the other marker were calculated (*B*). *C* and *D*, HEK293 cells expressing mCherry-Gal3 were treated with CPPs for 4 h, fixed, and stained with an anti-LAMP1 antibody (*C*). The percentages of Gal3- or LAMP1-positive dots that were also positive for the other marker were calculated (*D*). *Scale bars*, 5 μm (*A*) and 10 μm (*C*). *Arrows* indicate puncta positive for both markers. *Error bars*, S.E.

somal markers that were colocalized with Gal3 signals. We found that CPP-induced Gal3-positive puncta colocalized with the later endosome marker, Rab7 (Fig. 7, *A* and *B*), but not with the early endosome marker, Rab5 (data not shown). Almost all Gal3-positive vesicles expressed Rab7, and >75% of Rab7-positive vesicles were Gal3-positive in CPP-treated cells. The results suggested that the damage as defined by Gal3 positivity was most widely exhibited at the later endosome stage. Interestingly, we have also observed that most of the Gal3 puncta were colocalized with LAMP1, although only a smaller percentage of LAMP1 puncta was positive for Gal3 (Fig. 7, *C* and *D*). LAMPs are transported to the later endosomes from trans-Golgi network (26), and thus LAMP-positive compartments could represent the lysosome as wells as the intermediate compartment between the later endosome and the lysosome. Thus, CPP-induced endosomal damage/Gal3 positivity could include the later endosome, the lysosome, and the intermediate compartment.

We had observed previously that CPP-induced LC3-TVS could colocalize with Rab7 (6). We further found that most of the LC3-TVS were positive for LAMP1 (Fig. 8, *A* and *B*). Remarkably, we observed that the majority of LC3-TVS (nearly 80%) and LAMP-positive compartment (about 70%) were unable to degrade DQ-BSA because only a small fraction (20–30%) of these compartments showed DQ-BSA signals (Fig. 8, *C–E*). This suggested that these compartments did not have the degradation capacity, either because they represented the nondegradative later endosomes or because they were damaged to lose the acidic property as indicated in an early study (11). This notion would be consistent with additional observations made in this study, including that a smaller portion of LAMP positive-compartments (Fig. 8*B*) or DQ-BSA-positive compartments (Fig. 8*D*) were positive for LC3 because the larger portion of these compartments would represent normal undamaged vesicles.

Endosome Maturation Affects the Morphology of LC3-positive Autophagosomes—A significant feature of endosome maturation from the early to the later endosome is continuous acidification because of the increased expression of vacuolar-type H$^+$-ATPase (v-ATPase) (27). Blocking v-ATPase with BafA$_1$ or ConA inhibits endosome maturation to later endosomes and lysosomes (27–29) and caused LAMP-positive compartment swelling (Fig. 9*A*). We found that BafA$_1$ alone induced Gal3 recruitment (Fig. 9, *B* and *C*), indicating that this chemical caused endosome/lysosome damage as well. Cotreatment of CPPs seemed to enhance the swelling of LAMP1 compartment (Fig. 9*A*) without affecting the frequency of Gal3 signals (Fig. 9, *B* and *C*), suggesting that damage caused by either agent was sufficient to trigger Gal3 recruitment.
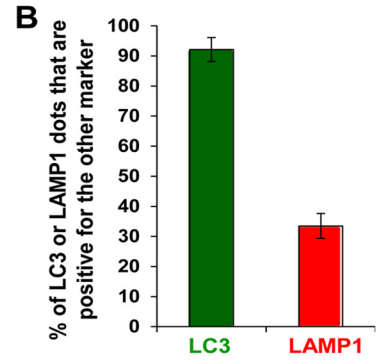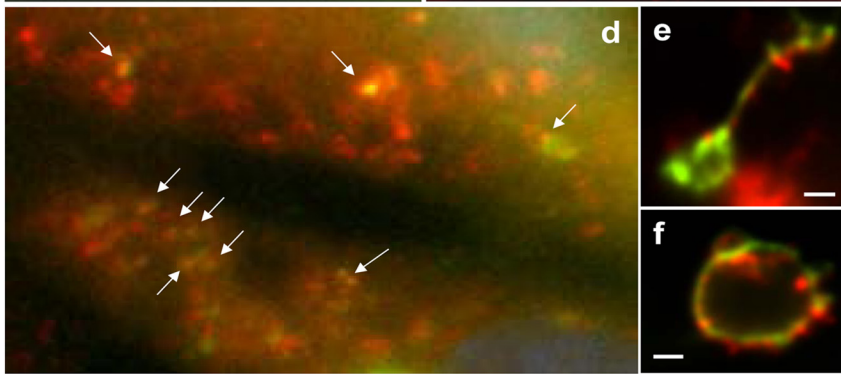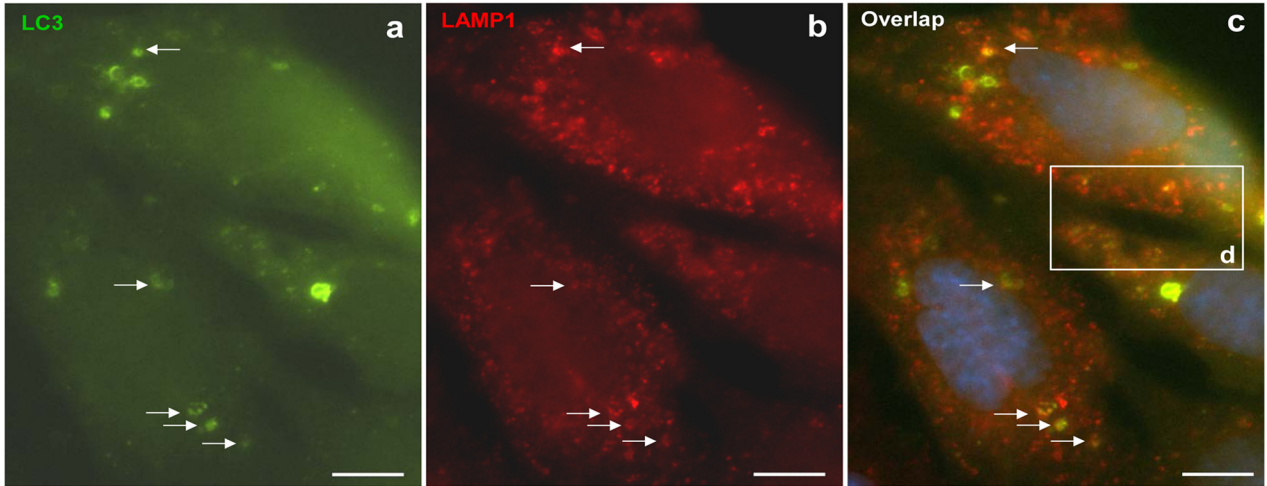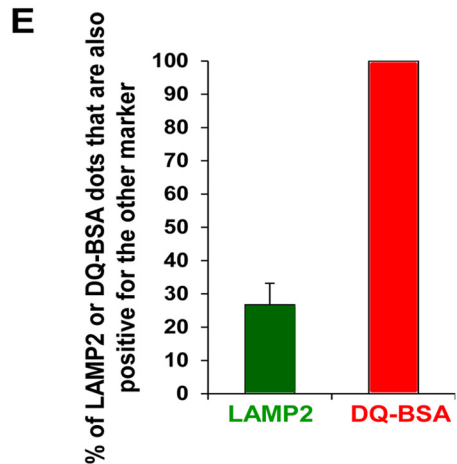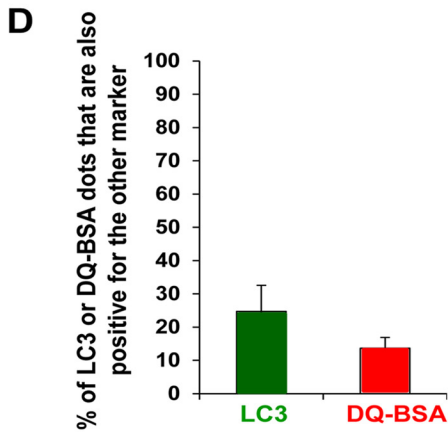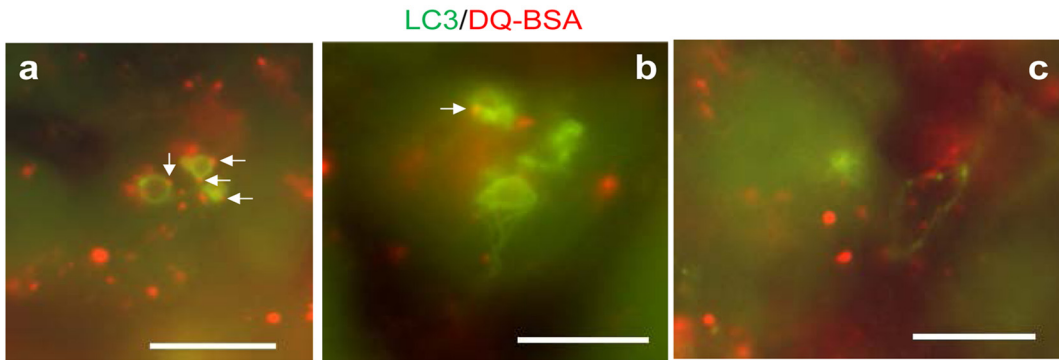
Paradoxically, CPP-induced LC3-TVS were significantly reduced by BafA$_1$ or ConA (Fig. 9, *D* and *E*). This effect seemed to be specific to the v-ATPase inhibitors because treatment with chloroquine or ammonium chloride was able to raise the pH of the acidic compartments but did not have the same effect of inhibiting the formation of LC3-TVS (Fig. 9, *D* and *E*). Inhibition of lysosome enzymatic activity with protease inhibitors E64D and pepstatin A had no effect either (data not shown).

Whereas CPP-induced LC3-TVS were inhibited by BafA$_1$, small regular-shaped LC3 puncta could still be observed in cells under high magnification (Fig. 9F). These puncta were much smaller in size and fainter in intensity and were not readily observed in cultures with CPPs alone, in which LC3-TVS were dominant. The data suggested that LC3-TVS might evolve from the smaller vesicles in a way dependent on v-ATPase and endosomal maturation.

DISCUSSION

CPP Treatment Causes Endosome Damage—Here we have shown that clathrin-mediated endocytosis is required for autophagy induction by CPPs. Another common transfection carrier, cationic liposomes, is also known to cause autophagy (30, 31), which was recently shown to be dependent on endocytosis as well (31).

Endocytosis, or phagocytosis, had been implicated in CPP-mediated DNA entry into cells (12, 13). Thus, it is consistent that the same process is important for CPPs to cause autophagy. How endocytosis is coupled to the canonical autophagy machinery is not known. Certainly not all agents endocytosed into cells may cause autophagy. Thus, CPPs or cationic lipids must trigger specific signaling pathways that are not shared by other nonautophagic endocytosed agents. In previous work we found that mTOR down-regulation and endoplasmic reticulum stress, commonly seen in autophagic conditions, were not involved in CPP-induced autophagy (7). However, endoplasmic reticulum membranes seem to contribute to the biogenesis of CPP-induced autophagosomes (7). Future works will have to be directed to dissect this link connecting endocytosis to autophagy induction.

Surprisingly, endocytosis of CPPs leads to endosomal damage, as indicated by the exposure of glycans that are recognized by Gal3. Gal3 binding was blocked when endocytosis was inhibited. We found that 90% of Gal3-positive vesicles were colocalized with filipin-positive membranes, suggesting that galectins were recruited mainly to endocytosed vesicles. The damaged vesicles are likely those that contain CPPs or CPP-DNA complex as DNA could be visualized in Gal3-positive vesicles (Fig. 4A). CPPs are thus damaging agents to the endosomal membrane.

Intracellular bacteria induced endosomal damage when entering cells by endocytosis/phagocytosis (22, 23). It has also been found that osmotic shock triggered endosome damage as indicated by galectin recruitment (23). Most recently, it was demonstrated that lysosomal damage caused by certain lysosomotropic agents was also characterized by galectin recruitment (11). Thus, endosomal damage could be induced by a variety of means. Endosomal damage caused by sterile agents, such as CPPs, may constitute a useful model for studying endosomal damage caused by infectious agents.

Interaction of the Damaged Endosomes with LC3-positive Autophagosomal Membranes—In the current and previous studies (11, 23), galectin-positive endosomes were found to colocalize with LC3-positive autophagosomes. Maejima *et al.* implicated that ubiquitin and p62 were involved in the interaction of autophagosomes with the damaged lysosomes (11). Ubiquitins have also been found to be conjugated to host cellular proteins in endosomes that contain *Salmonella*, which subsequently interact with several autophagic molecules, including Atg16L1, ULK1, and Atg9L (32).

We had found that overexpressed p62 were colocalized with CPP-induced LC3-TVS (6). In the present study using immunostaining we found that endogenous p62 was also strongly associated with LC3-TVS following CPP treatment (Fig. 5, *A* and *B*). Consistently, CPP-induced autophagy is accompanied by a significant degradation of p62 (4, 7). Concomitantly, LC3-TVS associated with ubiquitin signals were also increased following CPP treatment (Fig. 5, *C* and *D*). These results suggest a mechanism consistent with the classical selective autophagy in which target ubiquitination followed by target binding to p62 recruits autophagosomal membranes through this adaptor molecule (25). This hypothesis is strengthened with the finding that inhibition of p62 expression reduced LC3-TVS formation (Fig. 5).

The colocalization of Gal3-positive puncta with LC3-TVS further indicates that CPP-induced autophagosomes can recognize the damaged endosomes. Quantitative analysis indicated that as many as 90% of LC3-TVS were positive for filipin following CPP treatment, supporting the notion that most of the induced autophagosomes recognize endocytosed vesicles. A lower number of LC3-positive TVS were found to colocalize with Gal3-positive membranes, which varied depending on the methods used to detect the latter. This, together with the finding that only 60% of the filipin-positive puncta were positive for Gal3, suggests that other galectins, which could be also recognized by LC3, may be recruited to the endocytosed vesicles. Indeed, galectin 8 and galectin 9, but not galectin 1, have also been found to recognize glycans exposed on damaged vesicles caused by endocytosed bacteria (23). We suspect that a similar spectrum of galectin binding may occur in CPP treatment as suggested by the quantitative data.

FIGURE 8. **LC3-TVS are associated with the nondegradative endosomal compartment.** *A* and *B*, HEK293 cells expressing GFP-LC3 were treated with CPPs for 4 h, fixed, and stained with anti-LAMP1 followed by a Cy3-labeled secondary antibody. *Arrows* indicate puncta positive for both markers (*A*). A *boxed* area in *panel c* is enlarged in *panel d*. *Panels e* and *f* demonstrate the tubulovesicular nature of the puncta. The percentages of LC3- or LAMP1-positive puncta that were also positive for the other marker were calculated (*B*). *C* and *D*, HEK293 cells expressing GFP-LC3 were loaded with DQ-BSA for 2 h and then treated with CPPs for 4 h. *Arrows* indicate puncta positive for both markers (*C*). The percentages of LC3- or DQ-BSA-positive puncta that were also positive for the other marker were calculated (*D*). *E*, HEK293 cells were loaded with DQ-BSA for 2 h and then treated with CPPs for 4 h, fixed, and stained with anti-LAMP2. The percentages of LAMP2- or DQ-BSA-positive puncta that were also positive for the other marker were calculated. *Scale bars*, 5 μm (*A*) and 10 μm (*C*). *Error bars*, S.E.
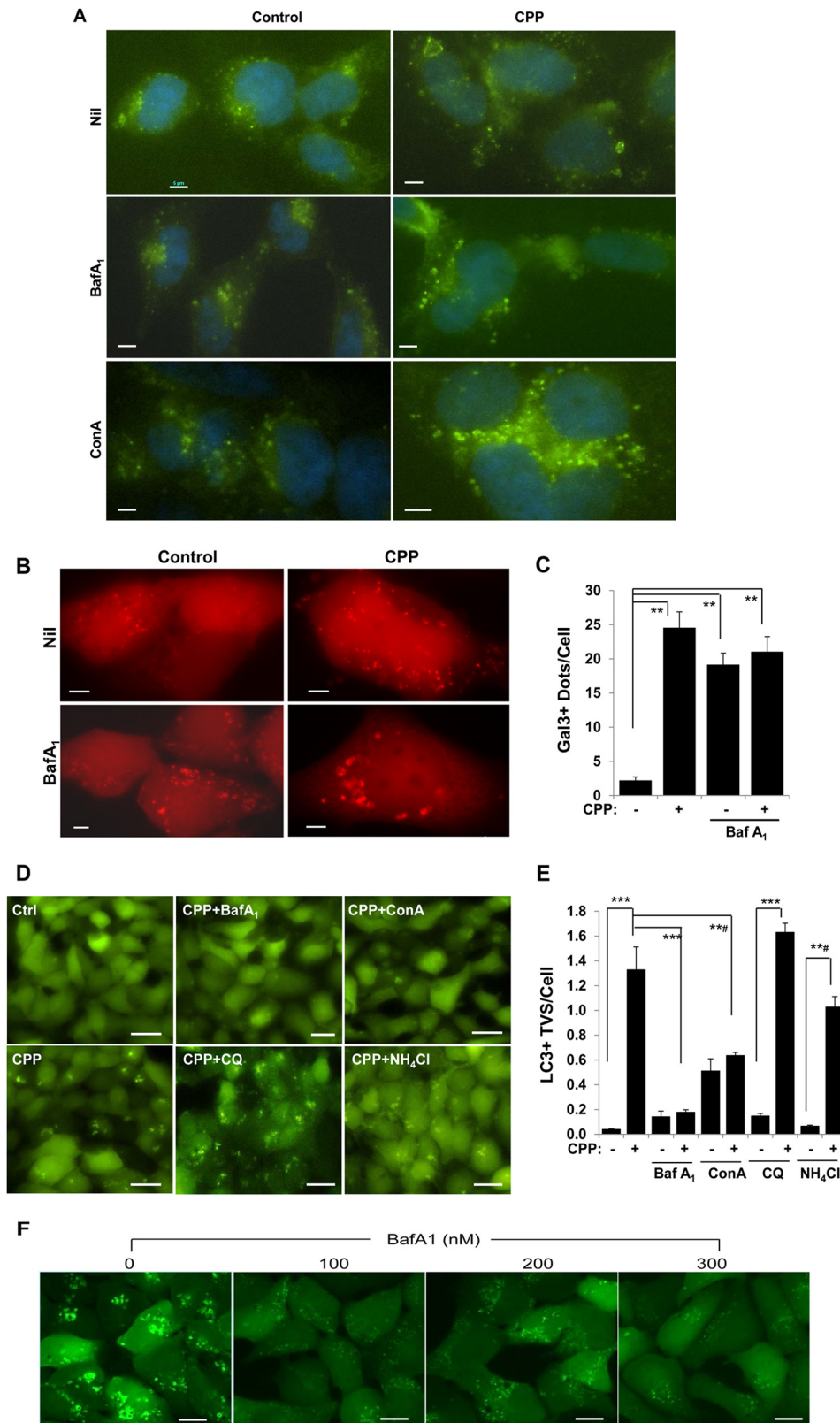
FIGURE 9. **v-ATPase inhibitors suppress CPP-induced LC3-TVS formation.** *A*, HEK293 cells were treated with CPPs in the presence or absence of BafA$_1$ (100 nM) or ConA (200 μM) for 4 h and stained for LAMP2. *B* and *C*, HEK293 cells expressing mCherry-Gal3 were treated as in *A*. Gal3-positive dots were imaged (*B*) and quantified (*C*). *D* and *E*, HEK293 cells expressing GFP-LC3 were treated with CPPs in the presence or absence of BafA$_1$, ConA, chloroquine, or NH$_4$Cl (*D*). The number of LC3-TVS per cell was quantified (*E*). *F*, HEK293 cells expressing GFP-LC3 were treated with CPPs in the presence of different concentrations of BafA$_1$ as indicated for 7 h. ***, $p < 0.001$; **#, $p < 0.002$; **, $p < 0.01$. *Scale bars*, 5 μm (*A* and *B*), 25 μm (*D*), and 10 μm (*F*). *Error bars*, S.E.

Galectin recruitment could initiate signaling events. Thurston *et al.* found that galectins bound to NDP52, which in turn bound to LC3, in a cellular bacterial infection model (23). Although we have found that CPP-induced LC3-TVS are colocalized with ubiquitin and p62, it has yet to be determined whether Gal3 can be ubiquitinated and whether p62 can interact directly with the ubiquitinated Gal3. However, inhibition of Gal3 expression reduced p62 puncta formation and LC3-TVS (Fig. 6), and inhibition of p62 expression further reduced LC3-TVS colocalization with Gal3 puncta (Fig. 5). These findings indicate that Gal3 is important in recruiting p62 and autophagosomal membranes to the damaged endosomes. The biochemical basis of these findings has yet to be elucidated in future studies.

Evolution of LC3-TVS Is Affected by v-ATPase Inhibitors—It seems that CPP-induced Gal3-positive endomembranes are mostly the later endosome and/or the lysosomes because Gal3-positive vesicles are mainly Rab7-positive or LAMP-positive (Fig. 7), with which LC3-TVS are associated as well (6) (Fig. 8). However, these compartments do not seem to be degradative, either because they are at the prelysosome stage (26, 27, 33) or because they are damaged and have lost the acidity and degradative capacity. The latter possibility is particularly noted in the study by Maejima *et al.* where direct lysosome damage was induced by lysosomotropic agents (11).

v-ATPase inhibitors, but not other types of lysosome inhibitors, could inhibit the formation of the tubulovesicular LC3-positive autophagosome. Small and faint LC3 puncta were not abundant in CPPs alone, where LC3-TVS dominated, but were abundant in the presence of BafA$_1$, where LC3-TVS disappeared, suggesting that LC3-TVS may evolve from the smaller puncta in a way relying on v-ATPase function or v-ATPase-dependent endosome/lysosome maturation.

Functional Implications of the Autophagosome-Endosome Interaction in CPP Treatment—An interesting but yet to be fully addressed issue is the significance of the interaction between the autophagosomes and the damaged endosomes. Thurston *et al.* have found that such interactions are important for the elimination of the endocytosed bacteria (23). Previous studies of anti-bacteria autophagy, or xenophagy, have suggested that autophagosomes can enwrap endocytosed bacteria for degradation (20, 21, 34). Ubiquitin conjugation in bacteria-containing endosomes has also been found to recruit autophagosomes that can lead to elimination of the bacteria (32). Whereas autophagosomes may recognize ubiquitinated bacteria directly, autophagosomes can also recognize the damaged endosomes containing the bacteria through the interaction with the galectins on the membrane (23) or ubiquitins conjugated to host cellular proteins (32). In the latter scenario, both bacteria and the damaged endosomes become the targets of the autophagosome. In a different scenario, interaction of autophagosomes with damaged lysosomes is also required for the autophagic removal of the latter (11).

Sterile damage of endosomes by CPPs or osmotic shock triggers a similar interaction with the autophagosome and may thus also represent a scenario in which autophagosomes recognize the damaged endosomes as autophagic targets. Interestingly, electron microscopy has shown that the content of CPP-induced autophagosomes was extensively membranous (4, 6). It is possible that in the case of sterile damage the functional significance of selective sequestration of damaged endosomes may be related to the homeostasis of the endosomal system.

An alternative explanation to the endosome-autophagosome interaction observed here is that the two compartments fuse to form a unique hybrid compartment. Such a fusion event has been proposed in earlier studies in mammalian cells, and the fused compartment is named as the amphisome (35, 36). Amphisome formation is thought to be beneficial as autophagosomes may in this way acquire the ability to fuse with the lysosome (36). This hypothesis is not supported in the anti-bacteria autophagy where electron microscopy can detect the presence of bacteria-containing vacuole within the double-membraned autophagosome (37). In addition, evidence for the fusion between autophagosomes and damaged lysosomes that expose glycans had not been found (11), but amphisome formation cannot be excluded in the CPP treatment condition even though CPP-induced double-membraned autophagosomes seem to contain membranous materials, which could be the damaged endosomes (4, 6). Similarly, amphisome formation cannot be excluded during the formation of LC3-TVS induced by cationic liposomes (31). Future studies should be directed to address this critical issue in the treatment with CPPs and cationic lipid agents.

Regardless of how the autophagosome interacts with the damaged endosome, it is well known that transfected DNA seemed to be largely brought to the lysosome for degradation (38–40). Notably, inhibition of either autophagy initiation or lysosome degradation could significantly increase the expression of DNA transfected with CPPs (38) or with cationic lipids (31). Thus, autophagy can serve as a defense mechanism against foreign DNA entering via the endosome system.

In summary, CPP treatment induced a significant level of endosomal damage, which may form the basis for the interaction between autophagosomes and the damaged endosomes. The unique interaction of the two vesicular systems may be important for the formation of the tubulovesicular autophagosomes and for their destiny. This system may provide a sterile model for studying anti-bacteria autophagy because of the similarity in the damage to endosomes and in the subsequent interaction with the autophagosomes.

REFERENCES

1. Mizushima, N., Levine, B., Cuervo, A. M., and Klionsky, D. J. (2008) Autophagy fights disease through cellular self-digestion. *Nature* **451,** 1069–1075
2. Tooze, S. A., and Yoshimori, T. (2010) The origin of the autophagosomal membrane. *Nat. Cell Biol.* **12,** 831–835
3. Graham, F. L., and van der Eb, A. J. (1973) A new technique for the assay of infectivity of human adenovirus 5 DNA. *Virology* **52,** 456–467
4. Gao, W., Ding, W. X., Stolz, D. B., and Yin, X. M. (2008) Induction of macroautophagy by exogenously introduced calcium. *Autophagy* **4,** 754–761
5. Sarkar, S., Korolchuk, V., Renna, M., Winslow, A., and Rubinsztein, D. C. (2009) Methodological considerations for assessing autophagy modulators: a study with calcium phosphate precipitates. *Autophagy* **5,** 307–313
6. Gao, W., Kang, J. H., Liao, Y., Ding, W. X., Gambotto, A. A., Watkins, S. C., Liu, Y. J., Stolz, D. B., and Yin, X. M. (2010) Biochemical isolation and characterization of the tubulovesicular LC3-positive autophagosomal

compartment. *J. Biol. Chem.* **285,** 1371–1383

7. Chen, X., Li, M., Chen, D., Gao, W., Guan, J. L., Komatsu, M., and Yin, X. M. (2012) Autophagy induced by calcium phosphate precipitates involves endoplasmic reticulum membranes in autophagosome biogenesis. *PLoS One* **7,** e52347

8. Ohsumi, Y., and Mizushima, N. (2004) Two ubiquitin-like conjugation systems essential for autophagy. *Semin. Cell Dev. Biol.* **15,** 231–236

9. Kabeya, Y., Mizushima, N., Ueno, T., Yamamoto, A., Kirisako, T., Noda, T., Kominami, E., Ohsumi, Y., and Yoshimori, T. (2000) LC3, a mammalian homologue of yeast Apg8p, is localized in autophagosome membranes after processing. *EMBO J.* **19,** 5720–5728

10. Loyter, A., Scangos, G. A., and Ruddle, F. H. (1982) Mechanisms of DNA uptake by mammalian cells: fate of exogenously added DNA monitored by the use of fluorescent dyes. *Proc. Natl. Acad. Sci. U.S.A.* **79,** 422–426

11. Maejima, I., Takahashi, A., Omori, H., Kimura, T., Takabatake, Y., Saitoh, T., Yamamoto, A., Hamasaki, M., Noda, T., Isaka, Y., and Yoshimori, T. (2013) Autophagy sequesters damaged lysosomes to control lysosomal biogenesis and kidney injury. *EMBO J.* **32,** 2336–2347

12. Loyter, A., Scangos, G., Juricek, D., Keene, D., and Ruddle, F. H. (1982) Mechanisms of DNA entry into mammalian cells. II. Phagocytosis of calcium phosphate DNA co-precipitate visualized by electron microscopy. *Exp. Cell Res.* **139,** 223–234

13. Orrantia, E., Li, Z. G., and Chang, P. L. (1990) Energy dependence of DNA-mediated gene transfer and expression. *Somat. Cell. Mol. Genet.* **16,** 305–310

14. Rodal, S. K., Skretting, G., Garred, O., Vilhardt, F., van Deurs, B., and Sandvig, K. (1999) Extraction of cholesterol with methyl-β-cyclodextrin perturbs formation of clathrin-coated endocytic vesicles. *Mol. Biol. Cell* **10,** 961–974

15. Subtil, A., Gaidarov, I., Kobylarz, K., Lampson, M. A., Keen, J. H., and McGraw, T. E. (1999) Acute cholesterol depletion inhibits clathrin-coated pit budding. *Proc. Natl. Acad. Sci. U.S.A.* **96,** 6775–6780

16. Nichols, B. (2003) Caveosomes and endocytosis of lipid rafts. *J. Cell Sci.* **116,** 4707–4714

17. Macia, E., Ehrlich, M., Massol, R., Boucrot, E., Brunner, C., and Kirchhausen, T. (2006) Dynasore, a cell-permeable inhibitor of dynamin. *Dev. Cell* **10,** 839–850

18. Ginsbach, C., and Fahimi, H. D. (1987) Labeling of cholesterol with filipin in cellular membranes of parenchymatous organs: standardization of incubation conditions. *Histochemistry* **86,** 241–248

19. Rich, K. A., Burkett, C., and Webster, P. (2003) Cytoplasmic bacteria can be targets for autophagy. *Cell Microbiol.* **5,** 455–468

20. Nakagawa, I., Amano, A., Mizushima, N., Yamamoto, A., Yamaguchi, H., Kamimoto, T., Nara, A., Funao, J., Nakata, M., Tsuda, K., Hamada, S., and Yoshimori, T. (2004) Autophagy defends cells against invading group A *Streptococcus*. *Science* **306,** 1037–1040

21. Amano, A., Nakagawa, I., and Yoshimori, T. (2006) Autophagy in innate immunity against intracellular bacteria. *J. Biochem.* **140,** 161–166

22. Paz, I., Sachse, M., Dupont, N., Mounier, J., Cederfur, C., Enninga, J., Leffler, H., Poirier, F., Prevost, M. C., Lafont, F., and Sansonetti, P. (2010) Galectin-3, a marker for vacuole lysis by invasive pathogens. *Cell Microbiol.* **12,** 530–544

23. Thurston, T. L., Wandel, M. P., von Muhlinen, N., Foeglein, A., and Randow, F. (2012) Galectin 8 targets damaged vesicles for autophagy to defend cells against bacterial invasion. *Nature* **482,** 414–418

24. Houzelstein, D., Gonçalves, I. R., Fadden, A. J., Sidhu, S. S., Cooper, D. N., Drickamer, K., Leffler, H., and Poirier, F. (2004) Phylogenetic analysis of the vertebrate galectin family. *Mol. Biol. Evol.* **21,** 1177–1187

25. Rogov, V., Dötsch, V., Johansen, T., and Kirkin, V. (2014) Interactions between autophagy receptors and ubiquitin-like proteins form the molecular basis for selective autophagy. *Mol. Cell* **53,** 167–178

26. Pols, M. S., van Meel, E., Oorschot, V., ten Brink, C., Fukuda, M., Swetha, M. G., Mayor, S., and Klumperman, J. (2013) hVps41 and VAMP7 function in direct TGN to late endosome transport of lysosomal membrane proteins. *Nat. Commun.* **4,** 1361

27. Huotari, J., and Helenius, A. (2011) Endosome maturation. *EMBO J.* **30,** 3481–3500

28. Clague, M. J., Urbé, S., Aniento, F., and Gruenberg, J. (1994) Vacuolar ATPase activity is required for endosomal carrier vesicle formation. *J. Biol. Chem.* **269,** 21–24

29. Bowman, E. J., Siebers, A., and Altendorf, K. (1988) Bafilomycins: a class of inhibitors of membrane ATPases from microorganisms, animal cells, and plant cells. *Proc. Natl. Acad. Sci. U.S.A.* **85,** 7972–7976

30. Man, N., Chen, Y., Zheng, F., Zhou, W., and Wen, L. P. (2010) Induction of genuine autophagy by cationic lipids in mammalian cells. *Autophagy* **6,** 449–454

31. Roberts, R., Al-Jamal, W. T., Whelband, M., Thomas, P., Jefferson, M., van den Bossche, J., Powell, P. P., Kostarelos, K., and Wileman, T. (2013) Autophagy and formation of tubulovesicular autophagosomes provide a barrier against nonviral gene delivery. *Autophagy* **9,** 667–682

32. Fujita, N., Morita, E., Itoh, T., Tanaka, A., Nakaoka, M., Osada, Y., Umemoto, T., Saitoh, T., Nakatogawa, H., Kobayashi, S., Haraguchi, T., Guan, J. L., Iwai, K., Tokunaga, F., Saito, K., Ishibashi, K., Akira, S., Fukuda, M., Noda, T., and Yoshimori, T. (2013) Recruitment of the autophagic machinery to endosomes during infection is mediated by ubiquitin. *J. Cell Biol.* **203,** 115–128

33. Dell'Angelica, E. C., Mullins, C., Caplan, S., and Bonifacino, J. S. (2000) Lysosome-related organelles. *FASEB J.* **14,** 1265–1278

34. Sumpter, R., Jr., and Levine, B. (2010) Autophagy and innate immunity: triggering, targeting and tuning. *Semin. Cell Dev. Biol.* **21,** 699–711

35. Berg, T. O., Fengsrud, M., Strømhaug, P. E., Berg, T., and Seglen, P. O. (1998) Isolation and characterization of rat liver amphisomes: evidence for fusion of autophagosomes with both early and late endosomes. *J. Biol. Chem.* **273,** 21883–21892

36. Eskelinen, E. L. (2005) Maturation of autophagic vacuoles in mammalian cells. *Autophagy* **1,** 1–10

37. Kageyama, S., Omori, H., Saitoh, T., Sone, T., Guan, J. L., Akira, S., Imamoto, F., Noda, T., and Yoshimori, T. (2011) The LC3 recruitment mechanism is separate from Atg9L1-dependent membrane formation in the autophagic response against *Salmonella*. *Mol. Biol. Cell* **22,** 2290–2300

38. Ege, T., Reisbig, R. R., and Rogne, S. (1984) Enhancement of DNA-mediated gene transfer by inhibitors of autophagic-lysosomal function. *Exp. Cell Res.* **155,** 9–16

39. Orrantia, E., and Chang, P. L. (1990) Intracellular distribution of DNA internalized through calcium phosphate precipitation. *Exp. Cell Res.* **190,** 170–174

40. Lechardeur, D., and Lukacs, G. L. (2002) Intracellular barriers to nonviral gene transfer. *Curr. Gene Ther.* **2,** 183–194